Characterization of intratumoral follicular helper T cells in follicular lymphoma: role in the survival of malignant B cells.

Patricia Amé-Thomas, Jérôme Le Priol, Hans Yssel, Gersende Caron, Céline Pangault, Rachel Jean, Nadine Martin, Teresa Marafioti, Philippe Gaulard, Thierry Lamy, et al.

Characterization of intratumoral follicular helper T cells in follicular lymphoma: role in the survival of malignant B cells

Patricia Amé-Thomas[1,2,3,4*], Jérôme Le Priol[1,2,3*], Hans Yssel[5], Gersende Caron[1,2,3,4], Céline Pangault[1,2,3,4], Rachel Jean[1,2,3,4], Nadine Martin[6,7], Teresa Marafioti[8], Philippe Gaulard[6,7], Thierry Lamy[1,2,3,4], Thierry Fest[1,2,3,4], Gilbert Semana[1,2,3] and Karin Tarte[1,2,3,4]

[1] INSERM, UMR 917, Rennes, F-35043, France

[2] Université Rennes 1, UMR 917, Rennes, F-35043, France

[3] Etablissement Français du Sang Bretagne, UMR 917, Rennes, F-35043, France

[4] Centre Hospitalier Universitaire (CHU) Rennes, F-35033, France

[5] INSERM, U844, Hôpital Saint-Eloi, Montpellier, F-34091, France

[6] INSERM, U955, Université Paris 12, Créteil, F-94010, France

[7] Hôpital Henri Mondor, Département de Pathologie, AP-HP, Créteil, F-94010, France

[8] University College Hospital, Department of histopathology, London, UK

*) P.A-T. and J.LP. contributed equally to this work

Running title: Intratumoral T_{FH} in follicular lymphoma

Corresponding author:

Pr. Karin TARTE

INSERM U917 - Faculté de médecine

2 Avenue du Pr Léon Bernard

35043 RENNES- France

e-mail: karin.tarte@univ-rennes1.fr

Phone: +33 2 23 23 45 12 / Fax:+33 2 23 23 49 58

ABSTRACT

Accumulating evidences indicate that the cellular and molecular microenvironment of follicular lymphoma (FL) plays a key role in both lymphomagenesis and patient outcome. Malignant FL B cells are found admixed to specific stromal and immune cell subsets, in particular $CD4^{pos}$ T cells displaying phenotypic features of follicular helper T cells (T_{FH}). The goal of our study was to functionally characterize intratumoral $CD4^{pos}$ T cells. We showed that $CXCR5^{hi}ICOS^{hi}CD4^{pos}$ T cells sorted from FL biopsies comprise at least two separate cell populations with distinct genetic and functional features: i) $CD25^{pos}$ follicular regulatory T cells (T_{FR}), and ii) $CD25^{neg}$ T_{FH} displaying a FL-B cell supportive activity without regulatory functions. Furthermore, despite their strong similarities with tonsil-derived T_{FH}, purified FL-derived T_{FH} displayed a specific gene expression profile including an overexpression of several genes potentially involved directly or indirectly in lymphomagenesis, in particular *TNF*, *LTA*, *IL4*, or *CD40LG*. Interestingly, we further demonstrated that these two last signals efficiently rescued malignant B cells from spontaneous and Rituximab-induced apoptosis. Altogether, our study demonstrates that tumor-infiltrating $CD4^{pos}$ T cells are more heterogeneous than previously presumed, and underlines for the first time the crucial role of T_{FH} in the complex set of cellular interactions within FL microenvironment.

Keywords: follicular lymphoma, follicular helper T cells, follicular regulatory T cells

INTRODUCTION

Follicular lymphoma (FL), the most frequent indolent non-Hodgkin lymphoma (NHL), results from the transformation of germinal center (GC) B cells (1). Besides a complex set of intrinsic genetic abnormalities, FL B cells retain, like their normal counterpart, a strong dependence on their molecular and cellular microenvironment. Indeed, malignant B cells are found admixed with specific stromal cell subsets (2) and $CD4^{pos}$ T cells (3), which form a specialized malignant cell niche within invaded lymphoid organs. Importantly, gene expression profile studies performed on whole tissue biopsies have revealed that the outcome of FL patients was not primarily predicted by the gene expression pattern of tumor B cells, but by gene signatures of non-malignant tumor infiltrating cells, with a favorable outcome related to T-cell restricted genes (4).

Several reports have confirmed that the nature and the localization of T cells within invaded lymph nodes (LN) could be used as prognostic biomarkers. Interestingly, the localization of $CD4^{pos}$ T cells within neoplastic follicles, unlike their absolute number, was consistently associated with poor survival and rapid transformation (5), suggesting that different $CD4^{pos}$ T cell subsets could display different functions in FL. Among them, regulatory T cells (Treg) are supposed to play a central role. Surprisingly, an increased number of $FOXP3^{pos}$ Treg has been first associated with improved overall survival (6). However, their follicular localization was thereafter associated with poor progression-free and overall survival, as well as a high risk of transformation (7). Furthermore, convincing functional studies revealed that natural and induced FL Treg were endowed with suppressive capacities towards infiltrating $CD4^{pos}$ effector T cells and $CD8^{pos}$ cytotoxic T cells (8-10). Overall, these data suggest that, like in solid tumors, Treg inhibit antitumor responses in FL. Other immunohistochemistry studies have focused on markers harbored by follicular helper T cells (T_{FH}), the specialized subset of $CD4^{pos}$ T cells present within secondary lymphoid organs (SLO). T_{FH} provide survival signals to antigen-selected GC B cells, and help them to achieve class-switch recombination and differentiation into antibody-secreting plasma cells. Highly controversial findings were reported concerning the prognostic value of the number and localization of $PD1^{pos}$ and $CD57^{pos}$ T cells (5, 11-13). However, the phenotypic definition of T_{FH} requires a combination of several markers thus limiting the impact of single marker-based

immunohistochemistry studies. In addition, whereas we recently identified a T_{FH}-dependent IL-4 centered pathway in FL, no functional study has been performed yet to explore the specific role of the T_{FH} compartment on malignant FL B cells.

T_{FH} are characterized by a strong expression of CXCR5 associated with a lack of CCR7 allowing their migration and retention into the CXCL13-rich light zone of GC. In addition, they express high levels of inducible costimulator (ICOS), CD200, PD-1, and produced IL-21 and CXCL13 (14). These features are essentially associated with the expression of the transcription factor BCL-6, the master regulator of T_{FH} differentiation (15). Importantly, T_{FH} subset has emerged as an independent $CD4^{pos}$ T helper lineage with distinct developmental program and effector functions. However, several recent reports revealed a higher plasticity within T helper lineages than previously anticipated. In particular, studies conducted in mice and humans demonstrated that T_{FH} could secrete IFN-γ, IL-4, and IL-17, the prototypic Th1, Th2, and Th17 cytokines (16-18).

Owing to the demonstration that, in both mice and human, CXCR5 and ICOS are two of the most relevant phenotypic T_{FH} cell markers (19, 20), we aimed to fully characterize $CXCR5^{hi}ICOS^{hi}CD4^{pos}$ T cells infiltrating FL tumors. In addition, since i) human tonsil $CD4^{pos}CD57^{pos}$ T_{FH} have been described to exert regulatory functions *in vitro* (21), and ii) Treg could localize within malignant follicles in FL (7) whereas they are essentially found in the extrafollicular zones in reactive lymph nodes (22), we decided to explore the relationship between T_{FH} and Treg in the FL context. We encompassed that the $CXCR5^{hi}ICOS^{hi}CD4^{pos}$ phenotypic definition merged two distinct functional T-cell populations in FL based on the expression of CD25: a $CD25^{pos}$ follicular Treg (T_{FR}) subset and a $CD25^{neg}$ T_{FH} subset. Finally, we demonstrated that FL-derived T_{FH} displayed a gene expression pattern close but distinct from that of tonsil-derived T_{FH} and exhibited a strong supportive activity on malignant FL B cells mediated in part by CD40L and IL-4.

MATERIALS AND METHODS

Cell samples

All tissues used for this study came from subjects recruited under institutional review board approval and informed consent process according to the Declaration of

Helsinki. Samples were obtained from LN of patients with *de novo* FL, diffuse large B-cell lymphoma (DLBCL), or with reactive non-malignant diseases considered as normal counterpart, and from tonsils collected from children undergoing routine tonsillectomy. All FL LN showed a predominant follicular growth pattern and were classified into grades 1, 2, or 3a according to the WHO diagnostic criteria. Tissues were cut into pieces and flushed using syringes and needles. The $CD4^{pos}$ T cell enriched fraction was obtained as previously described (17). T_{FH}, T_{FR}, and nonT_{FH} were sorted using a FACSAria (Becton Dickinson, San Diego, CA) as $CD3^{pos}CD4^{pos}CXCR5^{hi}ICOS^{hi}CD25^{neg}$, $CD3^{pos}CD4^{pos}CXCR5^{hi}ICOS^{hi}CD25^{pos}$, and $CD3^{pos}CD4^{pos}CXCR5^{neg}ICOS^{neg}$ cells, respectively. Purity of each fraction was greater than 98%. Primary FL B cells were purified as previously described (23). Purity of $CD19^{pos}$ B cells was greater than 99%, and more than 95% of these cells expressed the appropriate tumor isotype light chain. Magnetic cell sorts using the StemSep $CD4^{pos}$ T Cell Enrichment Kit (Stemcell Technologies, Vancouver, Canada) and the CD25 Microbeads II (Miltenyi Biotech, Gladbach, Germany) were performed to isolate $CD4^{pos}CD25^{neg}$ effector T cells from PBMC, and tonsil $CD4^{pos}CD25^{pos}$ cells required for the sorting of $CD4^{pos}CD25^{hi}CD127^{low}$ Treg. Th1, Th2, and Th17 clones were obtained from biopsies taken from active inflammatory lesions of patients suffering from chronic inflammatory or auto-immune diseases, as previously described (24).

Quantitative RT-PCR

Total RNA was extracted using RNeasy Kit (Qiagen, Valencia, CA). All samples used displayed an RNA integrity number of at least 9.4. cDNA was then generated using Superscript II reverse transcriptase (Invitrogen, Carlsbad, CA). For quantitative RT-PCR, we used assay-on-demand primers and probes (Table S1), and the Taqman Universal Master Mix from Invitrogen. Gene expression was measured using the ABI Prism 7000, or the ABI Prism 7900HT Sequence Detection System when predesigned TaqMan Array Micro Fluidic Cards were used. *B2M, CASC3*, and *18S* was determined as appropriate internal standard genes (25). For each sample, the C_T value for the gene of interest was determined, normalized to the geometric mean value of the 3 housekeeping genes, and compared to the value obtained from a pool of peripheral blood naive $CD4^{pos}$ T cells. A hierarchical clustering algorithm was used to group genes on the basis of similarity and data visualization was carried out with

Cluster and Treeview (Eisen softwares, Stanford, CA). Supervised analyses included two approaches: 1) Significance Analysis of Microarrays (SAM) software, using 500 permutations, a fold change > 2 or < 0.5 and an false discovery rate < 3%; 2) Unpaired Mann-Whitney non-parametric test carried out with Partek® Genomics Suite software (Partek, Saint Louis, MO), and selection of gene with a *P*-value less than 0.05. Generated gene lists were then crossed to retain only overlapping genes. Principal Component Analysis (PCA) was conducted using Partek® Genomics Suite.

Flow cytometry characterization

Monoclonal antibodies (mAbs) used are listed on Table S2. Data were analyzed using Kaluza software (Beckman Coulter, Miami, FL). For IL-4 and IFN-γ detection, total FL LN or tonsil cell suspensions were stimulated with 100 ng/mL of phorbol 12-myristate 13-acetate and 750 ng/mL of ionomycine for 6 hours in RPMI 10% fetal calf serum (FCS) at 37°C. Ten µg/mL of brefeldin A (BD Biosciences) were added for the last 4 hours of stimulation. The percentage of viable $CD3^{pos}$ T cells, nonT_{FH}, and T_{FH} producing IL-4 and IFN-γ was determined by staining with live/dead fixable yellow dead cell stain kit (Invitrogen) and cell-subset gating mAbs before fixation and permeabilization using the Cytofix/Cytoperm Fixation/Permeabilization Solution Kit (BD Biosciences) and incubation with anti IL-4 or anti-IFN-γ mAbs.

Immunohistochemistry studies

Immunohistochemistry was performed on deparaffinized tissue sections of FL LN, reactive LN with follicular hyperplasia, and tonsils using a standard indirect avidin-biotin immunoperoxidase method. Briefly, after appropriate antigen retrieval, sections were incubated with anti-human ICOS (provided by Dr T. Marafioti) and anti-human FOXP3 (clone 236A/E7 Abcam, Cambridge, UK) mAbs. Double immunostainings were performed as previously described (26). Images were captured with a Zeiss Axioskop2 microscope (Zeiss, Oberkochen, Germany) and Neofluar 100x/0.1 NA optical lenses (Zeiss). Photographs were taken with a DP70 Olympus camera (Olympus, Tokyo, Japan). Image acquisition was performed with Olympus DP Controller 2002, and images were processed with Adobe Photoshop v7.0 (Adobe Systems, San Jose, CA).

B-cell anti-apoptotic assay

Purified FL malignant B cells were cultured in IMDM 10% FCS in round bottom 96-well plates alone or in presence of purified T-cell subsets (ratio 1:1). After 24 hours, cells were harvested and B-cell apoptosis was assessed on gated $CD20^{pos}CD4^{neg}$ B cells using active caspase-3 PE apoptosis kit (Becton Dickinson), according to manufacturer's instructions. In addition, B-cell activation was evaluated in the same culture conditions after 40 hours of culture, by the ratio of the mean fluorescence intensity (RMFI) obtained with phycoerythrin-conjugated CD86 mAb and its isotype-matched negative control (Beckman Coulter).

Suppression assay

Effector T cells were stained with 5µM of carboxyfluorescein diacetate succinimidyl ester (CFSE, Invitrogen) and resuspended in IMDM 10% AB human serum (HS), 0.2 µg/mL anti-CD3 (Sanquin, Amsterdam, The Netherlands) and 0.1 µg/mL anti-CD28 (Becton Dickinson) mAbs. Cultures were performed in round bottom 96-well culture plates, in the presence or not of T_{FH}, nonT_{FH}, Treg, or T_{FR} (ratio of 1:1) for 5 days. $CFSE^{pos}TOPRO\text{-}3^{neg}$ viable effector T cells were analyzed. Percentages of cells in each generation were identified using the ModFit software (Verity Software, Topsham, ME).

Rituximab-induced cell death assay

Purified FL malignant B cells were plated in round bottom 96-well plates in IMDM 50% AB HS, and stimulated or not for 3 hours with 50 ng/mL CD40L, 35 ng/mL enhancer polyhistidine mAb, and 50 ng/mL IL-4 (RD Systems, Abingdon, UK) before 21 hours of culture in the presence or not of 25 µg/mL anti-CD20 mAb Rituximab (Mabthera™, Roche, Basel, Switzerland). The absolute number of $TOPRO\text{-}3^{neg}$ viable FL B cells was evaluated using Flowcount beads.

Statistical analyses

Statistical analyses were performed with the GraphPad Prism software using non-parametric Kruskal-Wallis test, Wilcoxon test for matched pairs, or Mann Whitney U tests.

RESULTS

Phenotypic description of CXCR5^{hi}ICOS^{hi}CD4^{pos} T cells in reactive and malignant secondary lymphoid organs

We first quantified by flow cytometry CXCR5^{hi}ICOS^{hi}CD4^{pos} T cells in dissociated samples of reactive LN and tonsils, as well as in infiltrated LN from patients with FL and *de novo* DLBCL. As previously described (17), we found a similarly high proportion of T_{FH} in tonsils (median: 30% [5-57]) and FL LN (median: 32% [10-57]). The percentage of CXCR5^{hi}ICOS^{hi} cells among CD4^{pos} T cells was low in the majority of reactive LN, with the exception of few samples with major follicular hyperplasia, as evaluated by morphological analysis of tissue sections. Interestingly, T_{FH} were not detected in the majority of DLBCL samples (median: 0.2% [0-20]) (Figure 1A). PD-1 is another well-known T_{FH} marker (14). Interestingly, whereas the percentage of T_{FH} among CD4^{pos} T cells was the same using both the CXCR5^{hi}ICOS^{hi} and the CXCR5^{hi}PD-1^{hi} definitions in tonsils, the percentage of CXCR5^{hi}PD-1^{hi}CD4^{pos} T cells represented only 78.8 ± 21% of that of CXCR5^{hi}ICOS^{hi}CD4^{pos} T cells in FL, suggesting an additional level of heterogeneity within CXCR5^{hi}ICOS^{hi}CD4^{pos} T-cell subset in this disease (Figure 1B).

Because previous data suggested that Treg could be specifically recruited in follicles in FL context (9), we also decided to characterize more precisely this population. We evaluated the expression of CD25 and FOXP3 among CD4^{pos} T cells within SLO. We revealed a higher frequency of FOXP3^{pos}CD25^{pos} Treg among CD4^{pos} T cells in FL, compared to tonsils, reactive LN, and DLBCL samples (Figure 1C). Interestingly, we noticed that FL LN samples were particularly enriched for CD4^{pos} T cells harbouring both CXCR5^{hi}ICOS^{hi} and FOXP3^{pos}CD25^{pos} phenotypes and were called thereafter follicular regulatory T cells (T_{FR}) (Figure 2A). In order to evaluate if this phenotype was really associated to a follicular localization, double-immunostainings were performed on FL biopsies and confirmed the presence of numerous FOXP3^{pos} cells co-expressing ICOS essentially within FL neoplastic follicles (Figure 3A). On the contrary, these cells were rare in GC of follicular hyperplasia, and were localized in the interfollicular areas or at the periphery of GC (Figure 3B), in accordance with their homogeneous low expression of CXCR5 in tonsils (Figure 2B). Finally, whereas no correlation was found between the proportions of total Treg and T_{FR} in FL samples,

we revealed a strong correlation between FL T_{FR} and T_{FH} contents (p=0.02) (Figure 2C).

Overall, we pointed out three $CD4^{pos}$ T-cell subsets in FL LN: classical $CD4^{pos}CXCR5^{hi}ICOS^{hi}CD25^{neg}FOXP3^{neg}$ T_{FH}, classical $CD4^{pos}CXCR5^{neg}ICOS^{neg}CD25^{pos}FOXP3^{pos}$ Treg, and a new $CD4^{pos}CXCR5^{hi}ICOS^{hi}CD25^{pos}FOXP3^{pos}$ T_{FR} compartment.

Definition of $CXCR5^{hi}ICOS^{hi}CD4^{pos}$ T cells in FL LN

To further explore the complexity of follicular $CD4^{pos}$ T cells in FL, we compared by quantitative RT-PCR, the gene expression profile of *ex-vivo* sorted Treg, FL-derived T_{FR}, and FL- and tonsil-derived T_{FH}. We also included in our analysis Th1, Th2, and Th17 clones derived from chronically inflamed human tissues that were shown to be highly representative of T-cell polarization in humans (24, 27). This study involved 45 genes that play a pivotal role in $CD4^{pos}$ T cell differentiation, localization and effector functions (Table S1). The results of a PCA analysis revealed that FL and tonsil-derived T_{FH} shared a very close gene expression signature, compared to Th1, Th2, Th17, Treg, and FL T_{FR} (Figure 4A). In addition, an unsupervised clustering analysis allowed to properly classify FL- and tonsil-derived T_{FH}, and ordered FL T_{FR} closer to Treg than T_{FH} (Figure 4B). More precisely, we then focused on the expression of the master regulators of each helper T-cell lineage, *i.e. TBX21*, *GATA3*, *RORC*, *FOXP3*, and *BCL6* involved and over-expressed during the Th1, Th2, Th17, Treg and T_{FH} cell differentiation, respectively. We confirmed that FL and tonsil-derived T_{FH} expressed lower to undetectable levels of *TBX21*, *GATA3*, and *RORC*, compared to Th1, Th2, and Th17. In addition, T_{FR} and Treg exhibited a similarly high level of *FOXP3*, unlike FL and tonsil-derived T_{FH}. FL- and tonsil-derived T_{FH} strongly expressed *BCL6* and were devoid of *PRDM1* expression, whereas FL T_{FR} strongly expressed *PRDM1* (Figure 4C). Overall, when focusing on T-helper differentiation genes, our data highlighted that FL-derived T_{FH} and T_{FR} shared a highly similar gene expression pattern with tonsil T_{FH} and Treg, respectively. However, T_{FR} retained a higher *BCL6* expression than classical Treg and the amount of *PDCD1* (encoding PD1) transcripts was intermediate in T_{FR}, as compared to T_{FH} and Treg. Finally, FL T_{FH} displayed the classical $PD\text{-}1^{hi}CD200^{hi}CD127^{low}CD57^{pos/neg}$ phenotype, previously ascribed to normal LN T_{FH}, whereas FL T_{FR} could be defined as $PD\text{-}1^{dim}CD200^{dim}CD127^{low}CD57^{pos/neg}CD4^{pos}$ T cells (Figure S1). These data were helpful to reconcile

the discrepancy, within FL biopsies, between the percentages of $CXCR5^{hi}CD4^{pos}$ T cells co-expressing high levels of ICOS (comprising T_{FH} and T_{FR}) *versus* high levels of PD-1 (comprising T_{FH} only) (Figure 1B) and confirmed that T_{FR} constitute a specific new cell subset distinct from both T_{FH} and Treg.

Functional characterization of $CXCR5^{hi}ICOS^{hi}CD4^{pos}$ T cells in FL LN

T_{FH} are defined by their capacity to support antigen-specific B-cell response by providing survival, activation, differentiation, and class switch recombination signals to normal B cells (14). We first explored malignant B cell activation and survival in coculture with $CD4^{pos}$ T-cell subsets. FL B cells upregulated the expression of the CD86 activation antigen when cultured with autologous T_{FH}, and not with $CXCR5^{neg}ICOS^{neg}CD4^{pos}$ nonT_{FH} (Figure 5A). Similarly, T_{FH}, unlike both nonT_{FH} and T_{FR}, were able to rescue autologous malignant B cells from spontaneous apoptosis *in vitro* (Figure 5B).

Furthermore, functional studies revealed that whereas T_{FR} did not display a malignant B-cell supportive effect, they exerted a strong regulatory potential, as demonstrated by their capacity to inhibit $CD4^{pos}CD25^{neg}$ effector T-cell proliferation as efficiently as tonsil Treg used as a control (Figures 5B-C). In the same experiment, paired FL T_{FH} displayed no regulatory properties (Figure 5C). These results convincingly demonstrated that T_{FR} could be considered as *bona fide* regulatory T cells expressing the GC specific receptor CXCR5.

In conclusion, our functional results convincingly demonstrated that, in FL, the $CXCR5^{hi}ICOS^{hi}CD4^{pos}$ T-cell definition included both functional $CXCR5^{hi}ICOS^{hi}CD25^{neg}CD4^{pos}$ T_{FH} with anti-apoptotic activity on autologous malignant B cells, and $CXCR5^{hi}ICOS^{hi}CD25^{pos}CD4^{pos}$ functional Treg.

CD40L/CD40 and IL-4/IL-4Rα are involved in FL B cell supportive activity of autologous T_{FH}

Despite the similarities between T_{FH} obtained from FL LN and tonsils, we next tried to unravel the specificity of T_{FH} in the malignant context. In fact, the unsupervised clustering analysis described above (Figure 4B) revealed some discrepancies between these two populations. Statistical analysis using combined SAM and Mann-Whitney U-test highlighted a significant differential expression of 10 genes, including 8 genes upregulated in FL-derived T_{FH} (Table 1). We focused our attention on 3 of

them: the B-cell activating cell surface molecule *CD40LG*, and the prototypic Th1 and Th2 cytokines, *IFNG* and *IL4*, previously reported as secreted by murine and human T_{FH} (17, 28, 29). We confirmed on a more important set of samples the significant over-expression of *CD40LG* and *IL4* in T_{FH} sorted from FL-LN, compared to those isolated from tonsils (Figure 6A). In addition, we found by flow cytometry that FL LN contained a higher frequency of IFN-γ secreting T cells than tonsils (median: 19.3% [14-32] and 10.8% [8-18] for FL LN and tonsils, respectively, $p<0.05$), in particular in the T_{FH} compartment (median 8.3% [6-22] and 4.5% [3-10], respectively, $p<0.05$) (Figure 6B). Similarly, the frequency of T cells secreting IL-4 was also more important in FL LN (median 12.7% [7-15]), as compared to tonsils (median 1.2% [1-3], $p<0.01$), and this cytokine was predominantly produced by the T_{FH} subset (Figure 6C). Taken together, these results prompted us to evaluate the role of CD40L and IL-4, two molecules implicated in normal B-cell growth, in the supportive effect of FL T_{FH}.

In order to answer this question, we first cultured FL LN samples in the presence of anti-CD40L and/or anti-IL-4Rα neutralizing mAbs, and evaluated the survival of malignant FL B cells. We were able to detect a slight but significant inhibition of malignant B-cell survival in the presence of each specific neutralizing antibody. Indeed, anti-CD40L and anti-IL-4Rα mAbs inhibited FL B cell survival by 11.5% [5.8-16.3] and 10.4% [1.6-11.5], respectively (n=4, data not shown). In order to better underline the direct anti-apoptotic activity of CD40L and IL-4 on FL B cells, we evaluated their impact on the survival of purified FL B cells, in the presence of the specific anti-CD20 mAb Rituximab, commonly used in the treatment of FL patients. These experiments were performed in the presence of human serum with an undamaged complement activity in order to evaluate the Rituximab-mediated complement-dependent cytotoxicity. Malignant B cells displayed a heterogeneous response to Rituximab cytotoxicity (median survival: 34%, [19-85]), as previously described (30). Nevertheless, whereas CD40L+IL-4 did not increase spontaneous FL B cell survival during short term culture, we observed a significant but highly variable decrease (median: 45%, [3-100], n=9) of Rituximab-dependent cytotoxicity in the presence of CD40L+IL-4 (Figure 6D). Overall, these results demonstrated that CD40L and IL-4, which are both overexpressed by FL-derived T_{FH}, contributed to FL B-cell survival.

DISCUSSION

FL B cells are characterized by chromosomal aberrations, a strong dependence on BCR signaling, and a bidirectional and dynamic crosstalk with both stromal and hematopoietic microenvironment within follicular malignant niche. Several studies using gene expression profile or immunohistochemistry approaches have depicted the importance of $CD4^{pos}$ T cells, depending on their number, activation status, and localization within malignant follicles (5, 12). To date, in FL, only few functional studies have been performed essentially focused on Treg. These data prompted us to better characterize follicular $CD4^{pos}$ T cells.

The primary goal of our study was to precisely define T_{FH} in FL samples. We identified a high proportion of $CXCR5^{hi}ICOS^{hi}CD4^{pos}$ T_{FH} in tonsils and reactive LN with a major follicular hyperplasia, correlated to the frequency of GC $CD10^{pos}$ B cells (data not shown), suggesting that T_{FH} cells might be related to the level and/or duration of follicular activation. LN obtained from FL and *de novo* DLBCL, the two most frequent NHL, showed adverse proportions of $CXCR5^{hi}ICOS^{hi}$ cells among $CD4^{pos}$ T cells, unrelated to the cancer-associated activation context. This observation reinforces the notion that FL cells might require stronger interactions with surrounding cells than DLBCL cells. Indeed, despite the influence of immune cell infiltration on DLBCL biology (31), clinical behaviour is primarily predicted by tumor cell molecular signatures in aggressive lymphomas (32), whereas FL patient outcome, including overall survival and risk of transformation, is essentially related to the gene signature of non-malignant infiltrating cells (4, 33). It will be interesting to evaluate the predictive value of T_{FH} cell infiltration in a large cohort of homogeneously treated FL patients.

Importantly, we demonstrated that $CXCR5^{hi}ICOS^{hi}CD4^{pos}$ T cells from FL LN comprised two distinct functional subpopulations, based on the expression of CD25 and FOXP3: *bona fide* $CD25^{pos}Foxp3^{pos}$ Treg called T_{FR}, and $CD25^{neg}FOXP3^{neg}$ T_{FH}. Natural Treg expressing ICOS have already been described in healthy donors (22). In melanoma, accumulating Treg expressing high levels of ICOS have been reported among tumor-infiltrating T cells. This $ICOS^{hi}$ Treg subset displayed strong suppressive functions, and induced the activation of IL-4-secreting T cells (34). In addition, we demonstrated the presence of these FL T_{FR} within neoplastic follicles, in accordance with their expression of CXCR5. The specific homing of Treg within

neoplastic GC could result from two complementary processes: their specific recruitment, or their local induction/expansion. Interestingly, CCL22 secreted by FL B cells has been described as involved in the recruitment of Treg (9), and previous data reported that malignant B cells contributed to Treg differentiation (35, 36). Importantly, two recent papers identify in mice a subset of $CXCR5^{hi}PD1^{hi}Foxp3^{pos}$ suppressive T cells that localize to the GC, coexpress *BCL6* and *PRDM1,* and arise from thymic-derived $Foxp3^{pos}$ precursors (37, 38). They called them T_{FR} cells. Our study provides strong evidence that this new T-cell population actually exists in human and is expanded during lymphomagenesis.

Here, we reported a strong correlation between T_{FR} and T_{FH} proportions, suggesting that CXCL13 secreted by T_{FH} could contribute to the recruitment of CXCR5-expressing T_{FR} within neoplastic follicles. In agreement, *CXCL13* was similarly highly expressed by tonsil and FL T_{FH} (data not shown). Of note, no correlation between expression of *CXCL13* and *FOXP3* within FL microenvironment (data not shown), or between the proportion of T_{FH} and total Treg have been found, reinforcing the specific relationship between T_{FH} and T_{FR}. Importantly, a recent report revealed the poor prognosis value of the follicular infiltration of $FOXP3^{pos}$ cells in FL biopsies (7). This may suggest that the T_{FR} subset plays an important role in FL pathogenesis through the inhibition of anti-tumor immune response. However, the low representation of T_{FR} in the FL microenvironment (median: 3% among $CD4^{pos}$ T cells) hampered us to perform more detailed functional investigations on this subset.

Beside this T_{FR} subpopulation, we demonstrated the presence of $CXCR5^{hi}ICOS^{hi}CD25^{neg}CD4^{pos}$ T cells sustaining FL B cell survival and activation, and therefore matching the functional definition of T_{FH}. In addition, this subset brought all the phenotypic features of human tonsil T_{FH}. We were able to show that FL T_{FH}, like tonsil T_{FH}, expressed less *TBX21*, *GATA3*, *RORC*, and *FOXP3* than Th1, Th2, Th17 clones, and natural Treg, and a higher *BCL6/PRDM1* ratio. FL and tonsil T_{FH} also expressed similar levels of *IL21*, and *BTLA*. Importantly, no regulatory function was associated to $CXCR5^{hi}ICOS^{hi}$ FL T_{FH}, contrary to previous data obtained with tonsil $CD57^{pos}$ T_{FH} (21). This apparent discrepancy may result from the different phenotypic definitions of T_{FH}. It has been demonstrated that CD57, unlike the CXCR5/ICOS combination, is not an appropriate marker of functional T_{FH} (20). In addition, we shown here that it could be more appropriate to define T_{FH} among

$CD4^{pos}CD25^{neg}$ T cells, as previously hypothesized (39), in order to reduce the potential contamination by Treg.

A more detailed analysis on selected genes revealed discrepancies between tonsil and FL T_{FH}. In particular, we demonstrated that FL-derived T_{FH} expressed more *IFNG*, *TNF,* and *LTA* than tonsil-derived T_{FH}. In a previous work, we reported an increased expression of these 3 genes in the entire microenvironment of FL B cells compared to normal tissues; and owing to the correlation between *IFNG, GRZA*, *GRZB,* and *CD8A* expression, we suggested the implication of cytotoxic cells in this secretion (23). Here, we demonstrated by quantitative RT-PCR experiments and flow cytometry strategies that T_{FH} were also involved in this overexpression of IFN-γ. Of note, this secretion of IFN-γ, TNF-α and LT-α by T_{FH} may have an influence on the FL B cell supportive effect of stromal cells, as described previously (23, 40). In addition, these inflammatory cytokines could also stimulate macrophages, which were shown to have an adverse effect on the outcome of FL patients (41, 42). We also observed an increased expression of the transcription factor aryl hydrocarbon receptor (AhR) in FL T_{FH}, compared to tonsil T_{FH}. AhR have been reported to regulate Th17, to induce the differentiation of Treg, and to enhance *CYP1A1*, *IL10*, or *IL22* expression (43-45). In the present study, gene expression data did not reveal an increased expression of these 3 genes in FL T_{FH}. However, it has also been reported that AhR could physically interact with c-Maf (43, 46), the transcription factor that specifically promotes IL-4 synthesis in Th2 cells. These two transcription factors could have a key role in the development and the functionality of IL4-producing T_{FH} in FL context.

Finally, FL T_{FH} showed an increased expression of three B-cell growth factors, *i.e*. *IL2*, *IL4* and *CD40LG*, compared to tonsil T_{FH}. Flow cytometry analyses revealed a higher proportion of IL-4 secreting cells within FL T_{FH}. The CD40/CD40L pathway is central to multiple steps of B-cell survival, activation, and differentiation. The growth activity of CD40L has already been demonstrated on neoplastic mature B cells (23) and IL-4 exerts an antiapoptotic activity on normal B cells (47, 48). Nevertheless, a dual role for IL-4 was demonstrated on DLBCL malignant cells, with an increased sensitivity of GCB-like DLBCL to doxorubicin and Rituximab, whereas IL-4 protected ABC-like DLBCL from drug-induced apoptosis (49). In addition, a previous report demonstrated that IL-4 slightly and irregularly enhanced the proliferation of FL B cells *in vitro* (50). In our study, we highlighted a strong anti-apoptotic activity of CD40L and

IL-4 on FL B cells treated *in vitro* with Rituximab. Interestingly, this anti-apoptotic effect was inversely correlated to the sensitivity of malignant FL B cells to Rituximab. Of note, beside its survival potential, IL-4 was also able to drive macrophages toward a TAM phenotype endowed with tumor invasion, immunoregulatory and pro-angiogenic properties (51).

In summary, our results depict new facets of the complex cellular interactions in FL and highlight the important supportive role of T_{FH} in the tumor microenvironment of FL malignant B cells. Targeting T_{FH} and their survival factors in combination with direct antitumor agents might be a promising strategy to provide new therapeutic schemes for FL patients.

ACKNOWLEDGMENTS

This work was supported by research fundings from the Association pour la recherche sur le cancer (ARC AO 2007), the Institut National du Cancer (INCa translationnel 2010; PLBIO-10-195), and the Association pour le Développement de l'Hémato-Oncologie (ADHO). JLP was supported by a PhD studentship from the Association Leucémie Espoir. The authors are indebted to the Centre de Ressources Biologiques (CRB)-Santé of Rennes hospital for its support in the processing of biological samples, the Institut Fédératif de Recherche (IFR) 140 of Rennes for cell sorting core facility, and Christophe Ruaux for providing tonsil samples.

CONFLICT OF INTEREST

The authors declare no conflict of interest.

Supplementary Information accompanies the paper on the Leukemia website (http://www.nature.com/leu)

REFERENCES

1. Shaffer AL, Rosenwald A, Staudt LM. Lymphoid malignancies: the dark side of B-cell differentiation. *Nat Rev Immunol* 2002 Dec; 2(12): 920-932.

2. Thomazy VA, Vega F, Medeiros LJ, Davies PJ, Jones D. Phenotypic modulation of the stromal reticular network in normal and neoplastic lymph nodes: tissue transglutaminase reveals coordinate regulation of multiple cell types. *Am J Pathol* 2003 Jul; 163(1): 165-174.

3. Carbone A, Gloghini A, Gruss HJ, Pinto A. CD40 ligand is constitutively expressed in a subset of T cell lymphomas and on the microenvironmental reactive T cells of follicular lymphomas and Hodgkin's disease. *Am J Pathol* 1995 Oct; 147(4): 912-922.

4. Dave SS, Wright G, Tan B, Rosenwald A, Gascoyne RD, Chan WC*, et al.* Prediction of survival in follicular lymphoma based on molecular features of tumor-infiltrating immune cells. *N Engl J Med* 2004 Nov 18; 351(21): 2159-2169.

5. Glas AM, Knoops L, Delahaye L, Kersten MJ, Kibbelaar RE, Wessels LA*, et al.* Gene-expression and immunohistochemical study of specific T-cell subsets and accessory cell types in the transformation and prognosis of follicular lymphoma. *J Clin Oncol* 2007 Feb 1; 25(4): 390-398.

6. Carreras J, Lopez-Guillermo A, Fox BC, Colomo L, Martinez A, Roncador G*, et al.* High numbers of tumor-infiltrating FOXP3-positive regulatory T cells are associated with improved overall survival in follicular lymphoma. *Blood* 2006 Nov 1; 108(9): 2957-2964.

7. Farinha P, Al-Tourah A, Gill K, Klasa R, Connors JM, Gascoyne RD. The architectural pattern of FOXP3-positive T cells in follicular lymphoma is an independent predictor of survival and histologic transformation. *Blood* 2010 Jan 14; 115(2): 289-295.

8. Yang ZZ, Grote DM, Ziesmer SC, Manske MK, Witzig TE, Novak AJ*, et al.* Soluble IL-2R{alpha} facilitates IL-2-mediated immune responses and predicts reduced survival in follicular B-cell non-Hodgkin lymphoma. *Blood* 2011, in press.

9. Yang ZZ, Novak AJ, Stenson MJ, Witzig TE, Ansell SM. Intratumoral CD4+CD25+ regulatory T-cell-mediated suppression of infiltrating CD4+ T cells in B-cell non-Hodgkin lymphoma. *Blood* 2006 May 1; 107(9): 3639-3646.

10. Yang ZZ, Novak AJ, Ziesmer SC, Witzig TE, Ansell SM. Attenuation of CD8(+) T-cell function by CD4(+)CD25(+) regulatory T cells in B-cell non-Hodgkin's lymphoma. *Cancer Res* 2006 Oct 15; 66(20): 10145-10152.

11. Alvaro T, Lejeune M, Salvado MT, Lopez C, Jaen J, Bosch R*, et al.* Immunohistochemical patterns of reactive microenvironment are associated with clinicobiologic behavior in follicular lymphoma patients. *J Clin Oncol* 2006 Dec 1; 24(34): 5350-5357.

12. Carreras J, Lopez-Guillermo A, Roncador G, Villamor N, Colomo L, Martinez A*, et al.* High numbers of tumor-infiltrating programmed cell death 1-positive regulatory lymphocytes are associated with improved overall survival in follicular lymphoma. *J Clin Oncol* 2009 Mar 20; 27(9): 1470-1476.

13. Richendollar BG, Pohlman B, Elson P, Hsi ED. Follicular programmed death 1-positive lymphocytes in the tumor microenvironment are an independent prognostic factor in follicular lymphoma. *Hum Pathol* 2011 Apr; 42(4): 552-557.

14. Crotty S. Follicular Helper CD4 T Cells (T(FH)). *Annu Rev Immunol* 2011 Apr 23; 29: 621-663.

15. Johnston RJ, Poholek AC, DiToro D, Yusuf I, Eto D, Barnett B*, et al.* Bcl6 and Blimp-1 are reciprocal and antagonistic regulators of T follicular helper cell differentiation. *Science* 2009 Aug 21; 325(5943): 1006-1010.

16. Ma CS, Suryani S, Avery DT, Chan A, Nanan R, Santner-Nanan B*, et al.* Early commitment of naive human CD4(+) T cells to the T follicular helper (T(FH)) cell lineage is induced by IL-12. *Immunol Cell Biol* 2009 Nov-Dec; 87(8): 590-600.

17. Pangault C, Ame-Thomas P, Ruminy P, Rossille D, Caron G, Baia M*, et al.* Follicular lymphoma cell niche: identification of a preeminent IL-4-dependent T(FH)-B cell axis. *Leukemia* 2010 Dec; 24(12): 2080-2089.

18. Bauquet AT, Jin H, Paterson AM, Mitsdoerffer M, Ho IC, Sharpe AH*, et al.* The costimulatory molecule ICOS regulates the expression of c-Maf and IL-21 in the development of follicular T helper cells and TH-17 cells. *Nat Immunol* 2009 Feb; 10(2): 167-175.

19. Akiba H, Takeda K, Kojima Y, Usui Y, Harada N, Yamazaki T*, et al.* The role of ICOS in the CXCR5+ follicular B helper T cell maintenance in vivo. *J Immunol* 2005 Aug 15; 175(4): 2340-2348.

20. Rasheed AU, Rahn HP, Sallusto F, Lipp M, Muller G. Follicular B helper T cell activity is confined to CXCR5(hi)ICOS(hi) CD4 T cells and is independent of CD57 expression. *Eur J Immunol* 2006 Jul; 36(7): 1892-1903.

21. Marinova E, Han S, Zheng B. Germinal center helper T cells are dual functional regulatory cells with suppressive activity to conventional CD4+ T cells. *J Immunol* 2007 Apr 15; 178(8): 5010-5017.

22. Ito T, Hanabuchi S, Wang YH, Park WR, Arima K, Bover L*, et al.* Two functional subsets of FOXP3+ regulatory T cells in human thymus and periphery. *Immunity* 2008 Jun; 28(6): 870-880.

23. Maby-El Hajjami H, Ame-Thomas P, Pangault C, Tribut O, DeVos J, Jean R*, et al.* Functional alteration of the lymphoma stromal cell niche by the cytokine context: role of indoleamine-2,3 dioxygenase. *Cancer Res* 2009 Apr 1; 69(7): 3228-3237.

24. Pene J, Chevalier S, Preisser L, Venereau E, Guilleux MH, Ghannam S*, et al.* Chronically inflamed human tissues are infiltrated by highly differentiated Th17 lymphocytes. *J Immunol* 2008 Jun 1; 180(11): 7423-7430.

25. Hamalainen HK, Tubman JC, Vikman S, Kyrola T, Ylikoski E, Warrington JA*, et al.* Identification and validation of endogenous reference genes for expression profiling of T helper cell differentiation by quantitative real-time RT-PCR. *Anal Biochem* 2001 Dec 1; 299(1): 63-70.

26. Bruneau J, Canioni D, Renand A, Marafioti T, Paterson JC, Martin-Garcia N*, et al.* Regulatory T-cell depletion in angioimmunoblastic T-cell lymphoma. *Am J Pathol* 2010 Aug; 177(2): 570-574.

27. Yssel H, De Vries JE, Koken M, Van Blitterswijk W, Spits H. Serum-free medium for generation and propagation of functional human cytotoxic and helper T cell clones. *J Immunol Methods* 1984 Aug 3; 72(1): 219-227.

28. Deenick EK, Chan A, Ma CS, Gatto D, Schwartzberg PL, Brink R*, et al.* Follicular helper T cell differentiation requires continuous antigen presentation that is independent of unique B cell signaling. *Immunity* 2010 Aug 27; 33(2): 241-253.

29. Reinhardt RL, Liang HE, Locksley RM. Cytokine-secreting follicular T cells shape the antibody repertoire. *Nat Immunol* 2009 Apr; 10(4): 385-393.

30. Manches O, Lui G, Chaperot L, Gressin R, Molens JP, Jacob MC*, et al.* In vitro mechanisms of action of rituximab on primary non-Hodgkin lymphomas. *Blood* 2003 Feb 1; 101(3): 949-954.

31. Monti S, Savage KJ, Kutok JL, Feuerhake F, Kurtin P, Mihm M*, et al.* Molecular profiling of diffuse large B-cell lymphoma identifies robust subtypes including one characterized by host inflammatory response. *Blood* 2005 Mar 1; 105(5): 1851-1861.

32. Alizadeh AA, Eisen MB, Davis RE, Ma C, Lossos IS, Rosenwald A*, et al.* Distinct types of diffuse large B-cell lymphoma identified by gene expression profiling. *Nature* 2000 Feb 3; 403(6769): 503-511.

33. de Jong D, de Boer JP. Predicting transformation in follicular lymphoma. *Leuk Lymphoma* 2009 Sep; 50(9): 1406-1411.

34. Strauss L, Bergmann C, Szczepanski MJ, Lang S, Kirkwood JM, Whiteside TL. Expression of ICOS on human melanoma-infiltrating

CD4+CD25highFoxp3+ T regulatory cells: implications and impact on tumor-mediated immune suppression. *J Immunol* 2008 Mar 1; 180(5): 2967-2980.

35. Yang ZZ, Novak AJ, Ziesmer SC, Witzig TE, Ansell SM. CD70+ non-Hodgkin lymphoma B cells induce Foxp3 expression and regulatory function in intratumoral CD4+CD25 T cells. *Blood* 2007 Oct 1; 110(7): 2537-2544.

36. Yang ZZ, Novak AJ, Ziesmer SC, Witzig TE, Ansell SM. Malignant B cells skew the balance of regulatory T cells and TH17 cells in B-cell non-Hodgkin's lymphoma. *Cancer Res* 2009 Jul 1; 69(13): 5522-5530.

37. Linterman MA, Pierson W, Lee SK, Kallies A, Kawamoto S, Rayner TF*, et al.* Foxp3(+) follicular regulatory T cells control the germinal center response. *Nat Med* 2011; 17(8): 975-982.

38. Chung Y, Tanaka S, Chu F, Nurieva RI, Martinez GJ, Rawal S*, et al.* Follicular regulatory T cells expressing Foxp3 and Bcl-6 suppress germinal center reactions. *Nat Med* 2011; 17(8): 983-988.

39. Lim HW, Kim CH. Loss of IL-7 receptor alpha on CD4+ T cells defines terminally differentiated B cell-helping effector T cells in a B cell-rich lymphoid tissue. *J Immunol* 2007 Dec 1; 179(11): 7448-7456.

40. Ame-Thomas P, Maby-El Hajjami H, Monvoisin C, Jean R, Monnier D, Caulet-Maugendre S*, et al.* Human mesenchymal stem cells isolated from bone marrow and lymphoid organs support tumor B-cell growth: role of stromal cells in follicular lymphoma pathogenesis. *Blood* 2007 Jan 15; 109(2): 693-702.

41. Byers RJ, Sakhinia E, Joseph P, Glennie C, Hoyland JA, Menasce LP*, et al.* Clinical quantitation of immune signature in follicular lymphoma by RT-PCR-based gene expression profiling. *Blood* 2008 May 1; 111(9): 4764-4770.

42. Clear AJ, Lee AM, Calaminici M, Ramsay AG, Morris KJ, Hallam S*, et al.* Increased angiogenic sprouting in poor prognosis FL is associated with elevated numbers of CD163+ macrophages within the immediate sprouting microenvironment. *Blood* 2010 Jun 17; 115(24): 5053-5056.

43. Gandhi R, Kumar D, Burns EJ, Nadeau M, Dake B, Laroni A*, et al.* Activation of the aryl hydrocarbon receptor induces human type 1 regulatory T cell-like and Foxp3(+) regulatory T cells. *Nat Immunol* 2010 Sep; 11(9): 846-853.

44. Quintana FJ, Basso AS, Iglesias AH, Korn T, Farez MF, Bettelli E*, et al.* Control of T(reg) and T(H)17 cell differentiation by the aryl hydrocarbon receptor. *Nature* 2008 May 1; 453(7191): 65-71.

45. Ramirez JM, Brembilla NC, Sorg O, Chicheportiche R, Matthes T, Dayer JM*, et al.* Activation of the aryl hydrocarbon receptor reveals distinct requirements for IL-22 and IL-17 production by human T helper cells. *Eur J Immunol* 2010 Sep; 40(9): 2450-2459.

46. Apetoh L, Quintana FJ, Pot C, Joller N, Xiao S, Kumar D*, et al.* The aryl hydrocarbon receptor interacts with c-Maf to promote the differentiation of type 1 regulatory T cells induced by IL-27. *Nat Immunol* 2010 Sep; 11(9): 854-861.

47. Illera VA, Perandones CE, Stunz LL, Mower DA, Jr., Ashman RF. Apoptosis in splenic B lymphocytes. Regulation by protein kinase C and IL-4. *J Immunol* 1993 Sep 15; 151(6): 2965-2973.

48. Wurster AL, Rodgers VL, White MF, Rothstein TL, Grusby MJ. Interleukin-4-mediated protection of primary B cells from apoptosis through Stat6-dependent up-regulation of Bcl-xL. *J Biol Chem* 2002 Jul 26; 277(30): 27169-27175.

49. Sarosiek KA, Nechushtan H, Lu X, Rosenblatt JD, Lossos IS. Interleukin-4 distinctively modifies responses of germinal centre-like and activated B-cell-like diffuse large B-cell lymphomas to immuno-chemotherapy. *Br J Haematol* 2009 Nov; 147(3): 308-318.

50. Schmitter D, Koss M, Niederer E, Stahel RA, Pichert G. T-cell derived cytokines co-stimulate proliferation of CD40-activated germinal centre as well as follicular lymphoma cells. *Hematol Oncol* 1997 Nov; 15(4): 197-207.

51. Gocheva V, Wang HW, Gadea BB, Shree T, Hunter KE, Garfall AL*, et al.* IL-4 induces cathepsin protease activity in tumor-associated macrophages to promote cancer growth and invasion. *Genes Dev* 2010 Feb 1; 24(3): 241-255.

FIGURE LEGENDS

Figure 1: Phenotypic characterization of $CD4^{pos}$ T cells in malignant and reactive SLO.

Frequency of $CXCR5^{hi}ICOS^{hi}$ **(A, B),** $CXCR5^{hi}PD\text{-}1^{hi}$ **(B),** and $FOXP3^{pos}CD25^{pos}$ **(C)** among $CD4^{pos}$ T cells from tonsils (Tons), reactive LN (rLN), FL LN, and DLBCL LN samples. (A) Open squares represent rLN samples with a strong follicular hyperplasia. Bars: median. *p<0.05; **p<0.001; ***p<0.0001.

Figure 2: Phenotypic characterization of FL T_{FR}.

(A) *Left:* Representative plots of CD25 and FOXP3 expression among $CXCR5^{hi}ICOS^{hi}CD4^{pos}$ T cells in FL. *Right:* Frequency of $CD25^{pos}FOXP3^{pos}$ subset among $CD4^{pos}CXCR5^{hi}ICOS^{hi}$ T cells from tonsils (Tons) and FL LN. **(B)** CXCR5 expression of $CD25^{pos}FOXP3^{pos}$ cells among $CD4^{pos}$ T cells in Tons and FL LN. **(C)** Correlation between the percentage of T_{FR}, and the percentages of Treg or T_{FH} in FL LN.

Figure 3: $FOXP3^{pos}ICOS^{pos}$ cells in FL LN and reactive SLO.

Immunohistochemistry in biopsies of **(A)** two cases of FL (1,2; respectively x100 and X400; 3,4; respectively X100 and X400), and **(B)** a reactive tonsil (1,2; respectively x100 and X250) and a LN with follicular hyperplasia (3,4; respectively X100 and X250). Double staining for FOXP3 (nuclear, blue) and ICOS (membrane, brown) show only very few cells expressing both markers in reactive tonsils and LN, mainly surrounding reactive GC (arrows) whereas a significant proportion of cells – either scattered or in small clusters - in the neoplastic follicles of FL are double stained for FOXP3 and ICOS.

Figure 4: Gene expression of FL T_{FH} and T_{FR}.

(A) PCA of data resulting from the gene expression analyses of Th1, Th2, Th17, Treg, tonsil-derived T_{FH} (Tons), FL-derived T_{FR} and T_{FH}. **(B)** Hierarchical clustering of Treg, FL T_{FH} and T_{FR}, and Tons T_{FH}. **(C)** *TBX21*, *GATA3*, *RORC*, *FOXP3*, *BCL6, PRDM1, and PDCD1* gene expression in FL T_{FH} and T_{FR}, and Tons T_{FH} were compared to that in Th1, Th2, Th17 and Treg (n=4 for Tons T_{FH}, FL T_{FH} and T_{FR}, n=3

for Th1, Th2, Th17, and Treg). The arbitrary value of 1 was assigned to blood naive $CD4^{pos}$ T cells. Bars: mean+/-SD.

Figure 5: Functional characterization of FL T_{FH} and T_{FR}.

(A,B) Purified FL B cells were cultured alone or with autologous T_{FH}, nonT_{FH}, or T_{FR}. **(A)** *Left:* representative plots of CD86 (line) or isotype-matched (grey) staining on gated B cells. *Right:* CD86 expression fold change after coculture with T_{FH} or nonT_{FH}. The RMFI for each coculture condition was compared to the RMFI of B cells cultured alone, allowing the calculation of the ratio of RMFI (RRMFI). Bars: mean+/-SD (n=3). **(B)** *Left:* representative plots of active caspase-3 staining on gated B cells. *Right:* Percentages of inhibition of B-cell apoptosis in coculture with T subsets. Bars: mean+/-SD (n=3). **(C)** Activated (A) or non-activated (NA) CFSE-labelled effector T cells (Teff) were cultured alone or in presence of Teff, Treg, or T_{FR}, T_{FH}, and nonT_{FH} isolated from FL LN. *Left:* representative plots of CFSE staining. *Right:* Bars: percentages of $CFSE^{pos}$ Teff displaying less (<G2, black) or more (• G2, white) than 2 cell divisions (n=3).

Figure 6: CD40L and IL-4 involvement in FL B-cell survival.

(A) *IL4* and *CD40LG* expression of Tons and FL T_{FH}. The arbitrary value of 1 was assigned to blood naive $CD4^{pos}$ T cells. Bars: mean+/-SD (n=6). *p<0.05, **p<0.01. **(B,C)** *Left:* representative plots of IFN-γ (B) or IL-4 (C) expression of activated (A) or non-activated (NA) $PD1^{pos}$ FL T_{FH}. *Right*: expression of IFN-γ (B) or IL-4 (C) by T_{FH} or $CD3^{pos}$ T cells from Tons or FL LN. Bars: median. *p<0.05, **p<0.01. **(D)** Relative number of viable FL B cells after culture in presence or not of Rituximab and CD40L+/-IL-4. Number of viable FL B cells obtained without CD40L+IL-4 and without Rituximab was assigned to 100. Bars: median (n=9). **p<0.01.

Table 1: List of the 10 genes differentially expressed by sorted FL T_{FH}, compared to tonsil (Tons) T_{FH}.

Gene Symbol	Median of expression in FL T_{FH}	Median of expression in Tons T_{FH}	Ratio of median expression (FL T_{FH} / Tons T_{FH})
IL4	**171.1**	**4.3**	**39.8**
IL2	76.4	3.4	22.3
IFNG	**10.1**	**1.8**	**5.5**
TNF	29.6	6.8	4.3
CD200	56.7	21.1	2.7
CD40LG	**6.5**	**2.5**	**2.6**
AHR	2.6	1.1	2.4
LTA	2.8	1.4	2.0
RORC	0.05	2.1	0.02
IL26	0.41	36.0	0.01

Figure 1

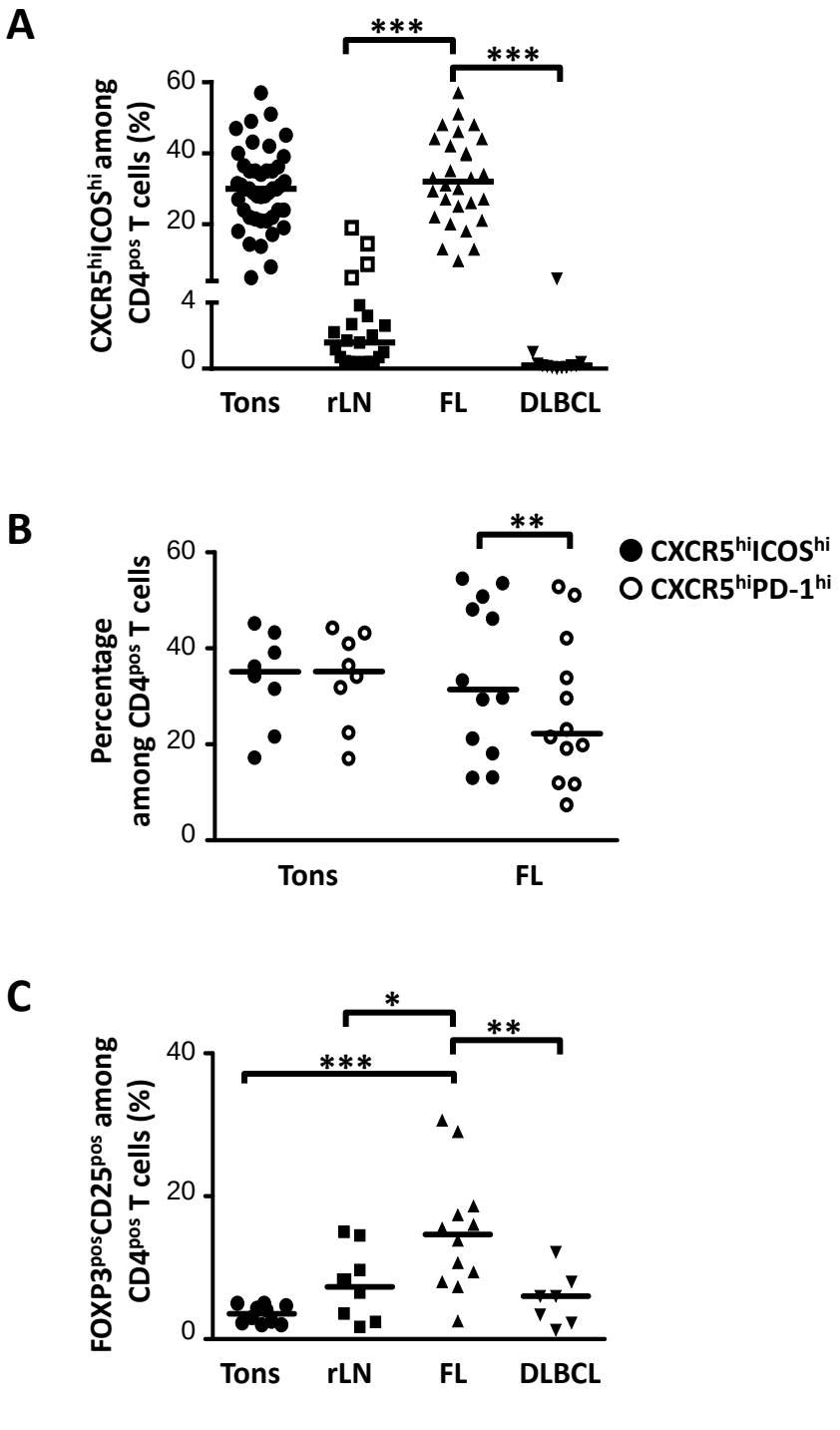
A
***
***
CXCR5hiICOShi among CD4pos T cells (%)
60
40
20
4
0
Tons
rLN
FL
DLBCL
B
**
Percentage among CD4pos T cells
60
40
20
0
Tons
FL
CXCR5hiICOShi
CXCR5hiPD-1hi
C
*
**
***
FOXP3posCD25pos among CD4pos T cells (%)
40
20
0
Tons
rLN
FL
DLBCL

Figure 2

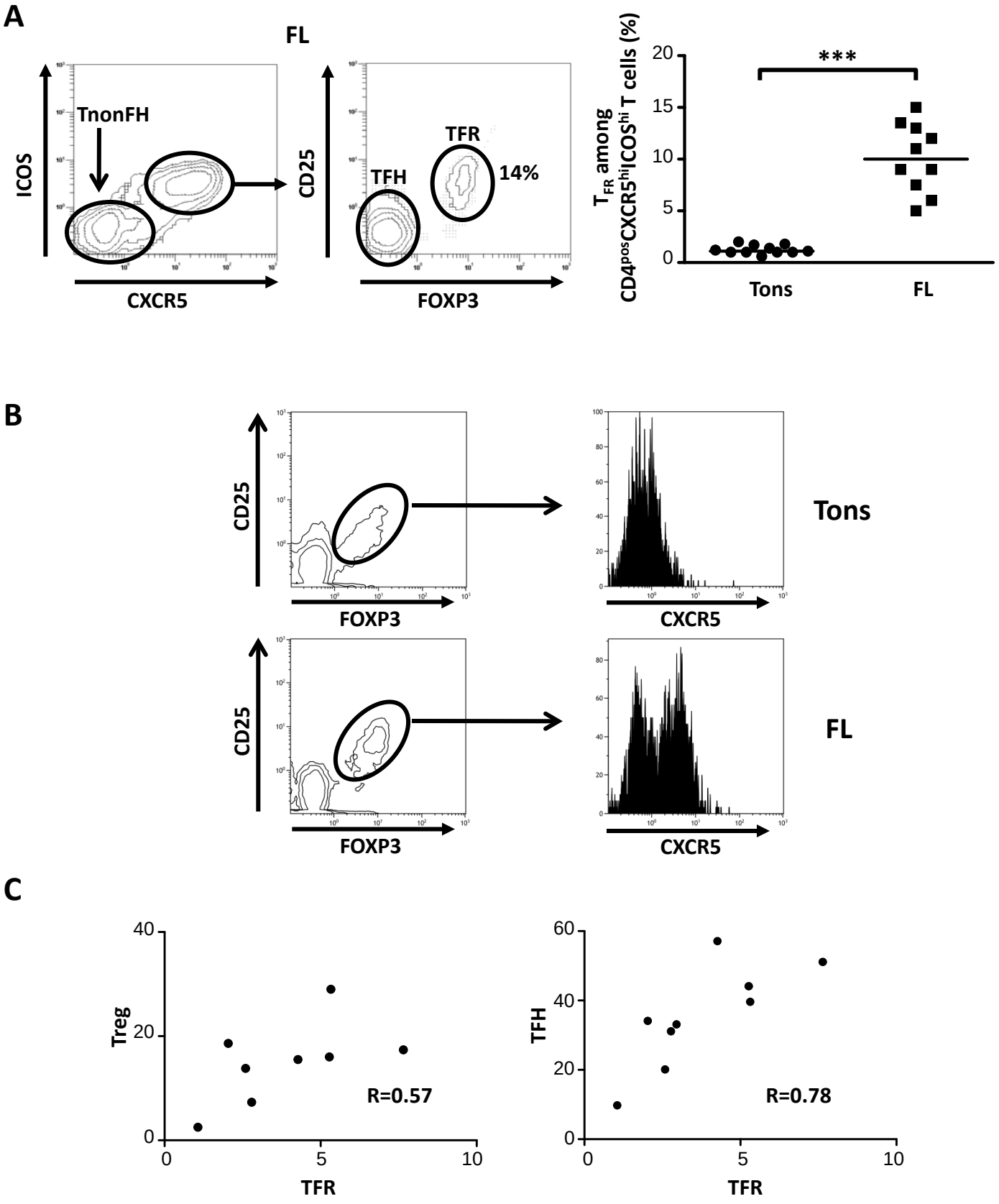
A
FL
TnonFH
ICOS
CXCR5
CD25
FOXP3
TFH
TFR
14%
T_{FR} among $CD4^{pos}CXCR5^{hi}ICOS^{hi}$ T cells (%)
***
Tons
FL
B
CD25
FOXP3
CXCR5
Tons
FL
C
Treg
TFR
R=0.57
TFH
R=0.78

Figure 3

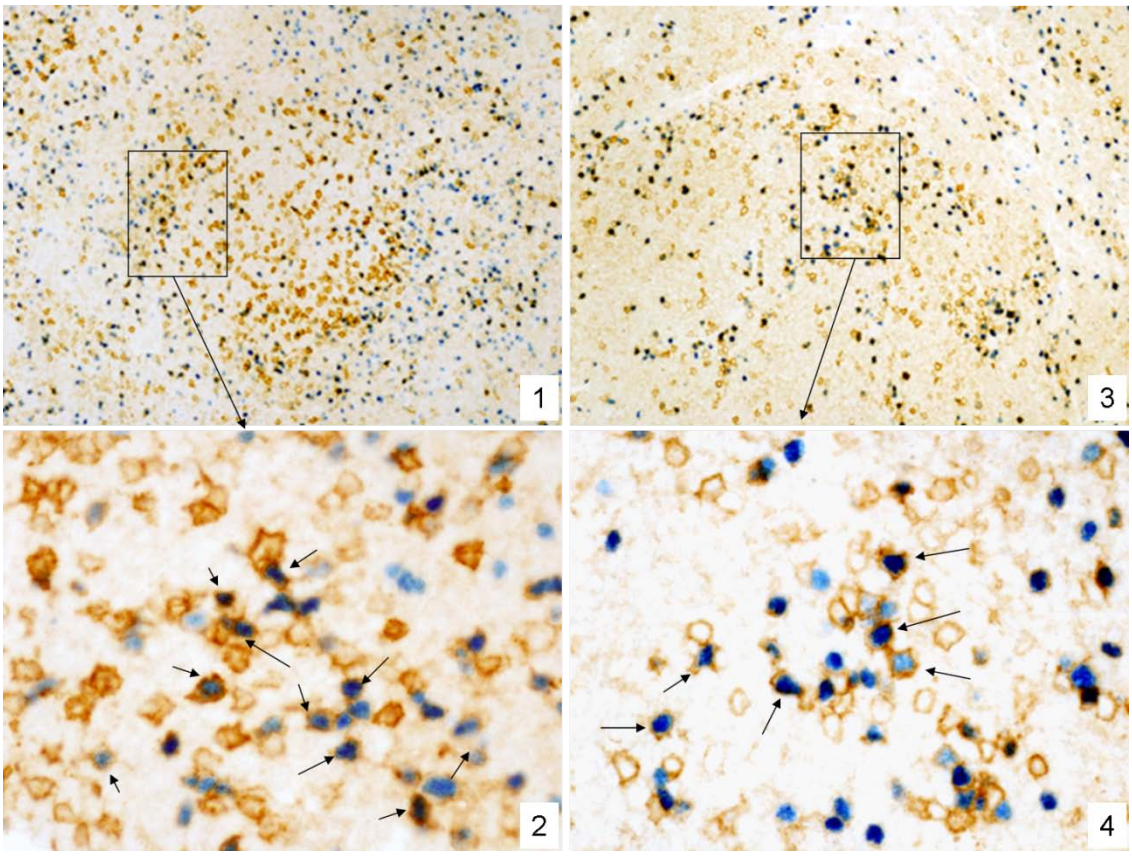

Figure 4

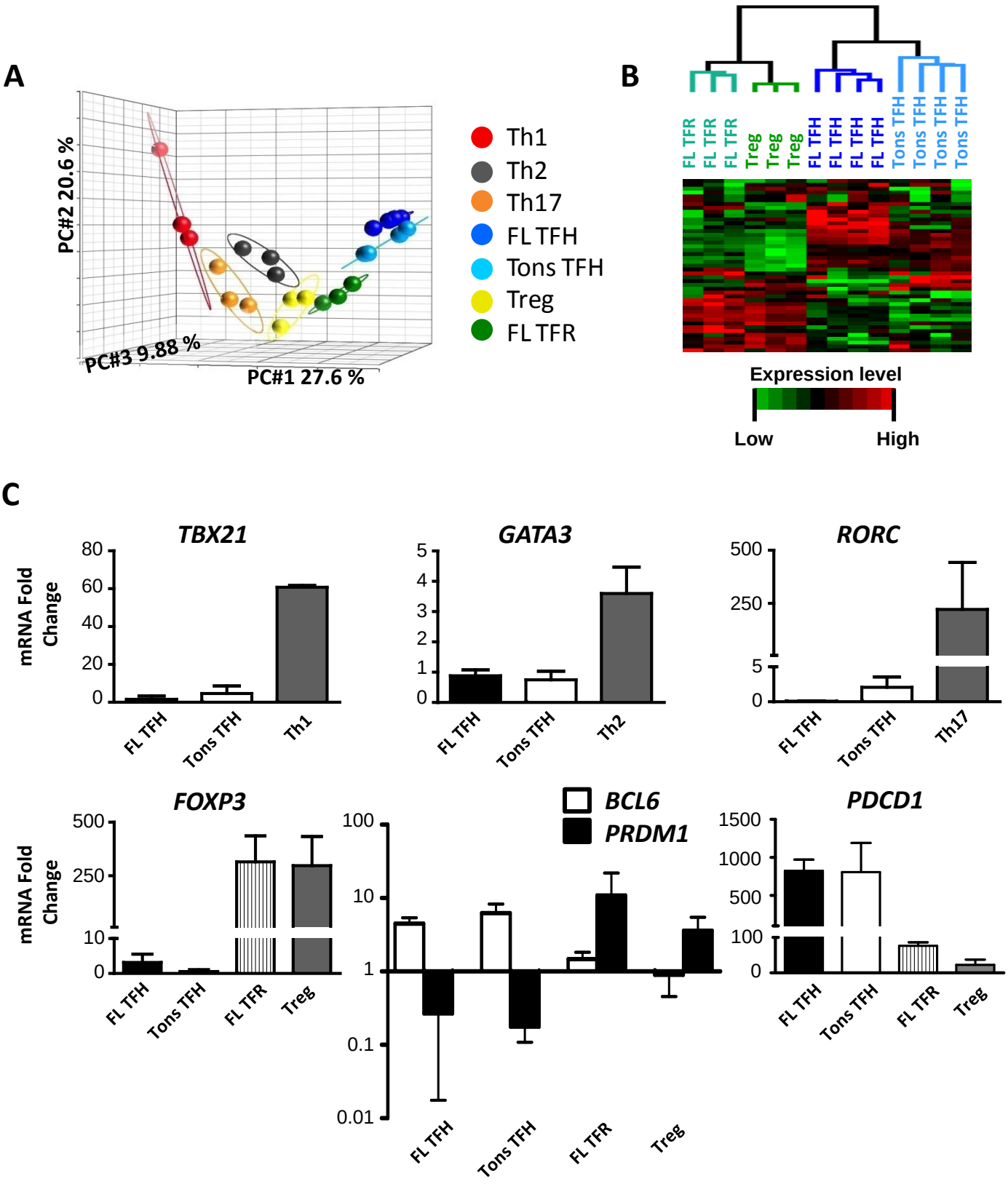
A
PC#2 20.6 %
PC#3 9.88 %
PC#1 27.6 %
Th1
Th2
Th17
FL TFH
Tons TFH
Treg
FL TFR
B
FL TFR
FL TFR
FL TFR
Treg
Treg
Treg
FL TFH
FL TFH
FL TFH
FL TFH
Tons TFH
Tons TFH
Tons TFH
Tons TFH
Expression level
Low
High
C
TBX21
mRNA Fold Change
80
60
40
20
0
FL TFH
Tons TFH
Th1
GATA3
5
4
3
2
1
0
FL TFH
Tons TFH
Th2
RORC
500
250
5
0
FL TFH
Tons TFH
Th17
FOXP3
mRNA Fold Change
500
250
10
0
FL TFH
Tons TFH
FL TFR
Treg
BCL6
PRDM1
100
10
1
0.1
0.01
FL TFH
Tons TFH
FL TFR
Treg
PDCD1
1500
1000
500
100
0
FL TFH
Tons TFH
FL TFR
Treg

Figure 5

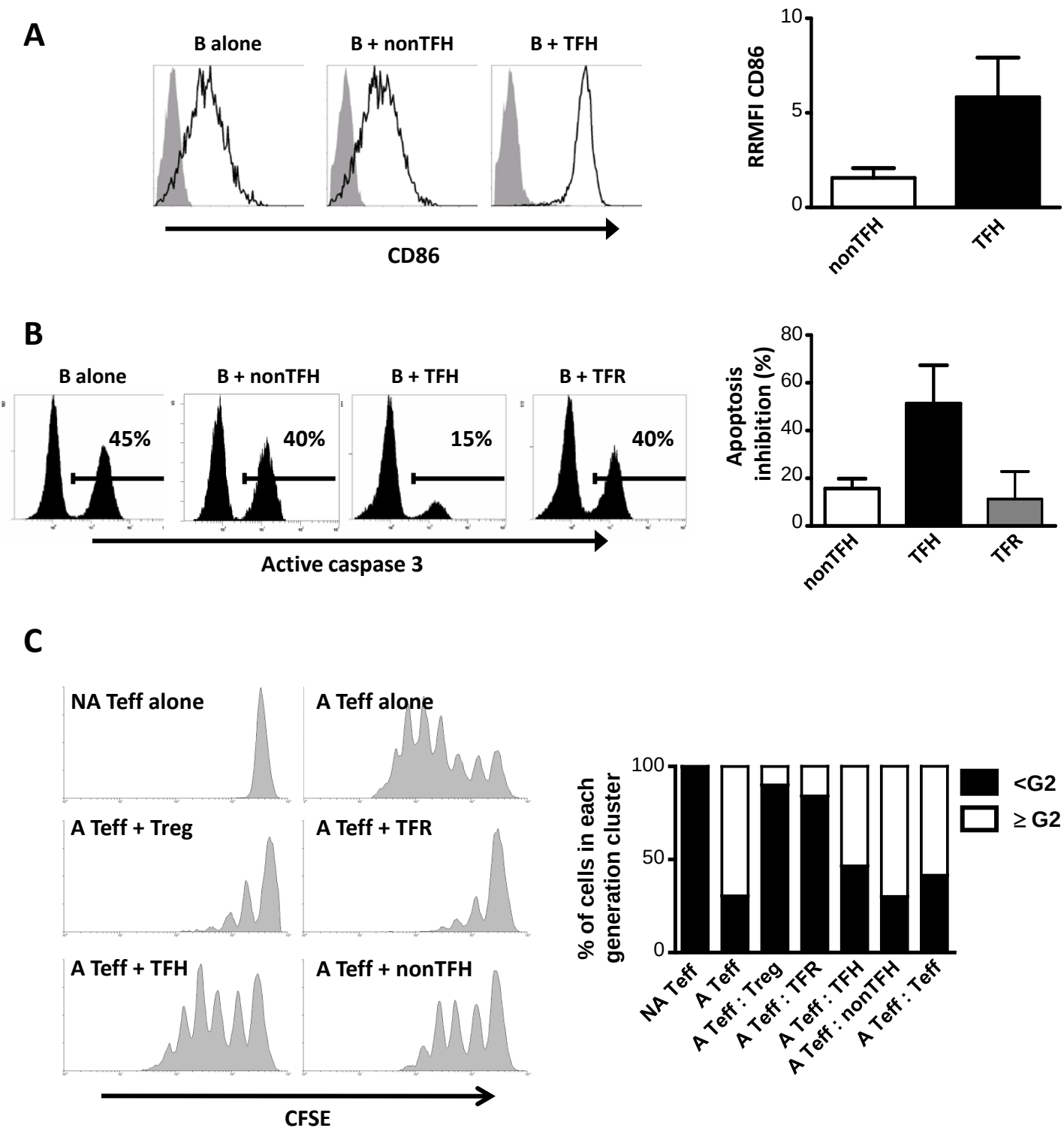
A
B alone
B + nonTFH
B + TFH
CD86
RRMFI CD86
10
5
0
nonTFH
TFH
B
B alone
B + nonTFH
B + TFH
B + TFR
45%
40%
15%
40%
Active caspase 3
Apoptosis inhibition (%)
80
60
40
20
0
nonTFH
TFH
TFR
C
NA Teff alone
A Teff alone
A Teff + Treg
A Teff + TFR
A Teff + TFH
A Teff + nonTFH
CFSE
% of cells in each generation cluster
100
50
0
<G2
≥ G2
NA Teff
A Teff
A Teff : Treg
A Teff : TFR
A Teff : TFH
A Teff : nonTFH
A Teff : Teff

Figure 6

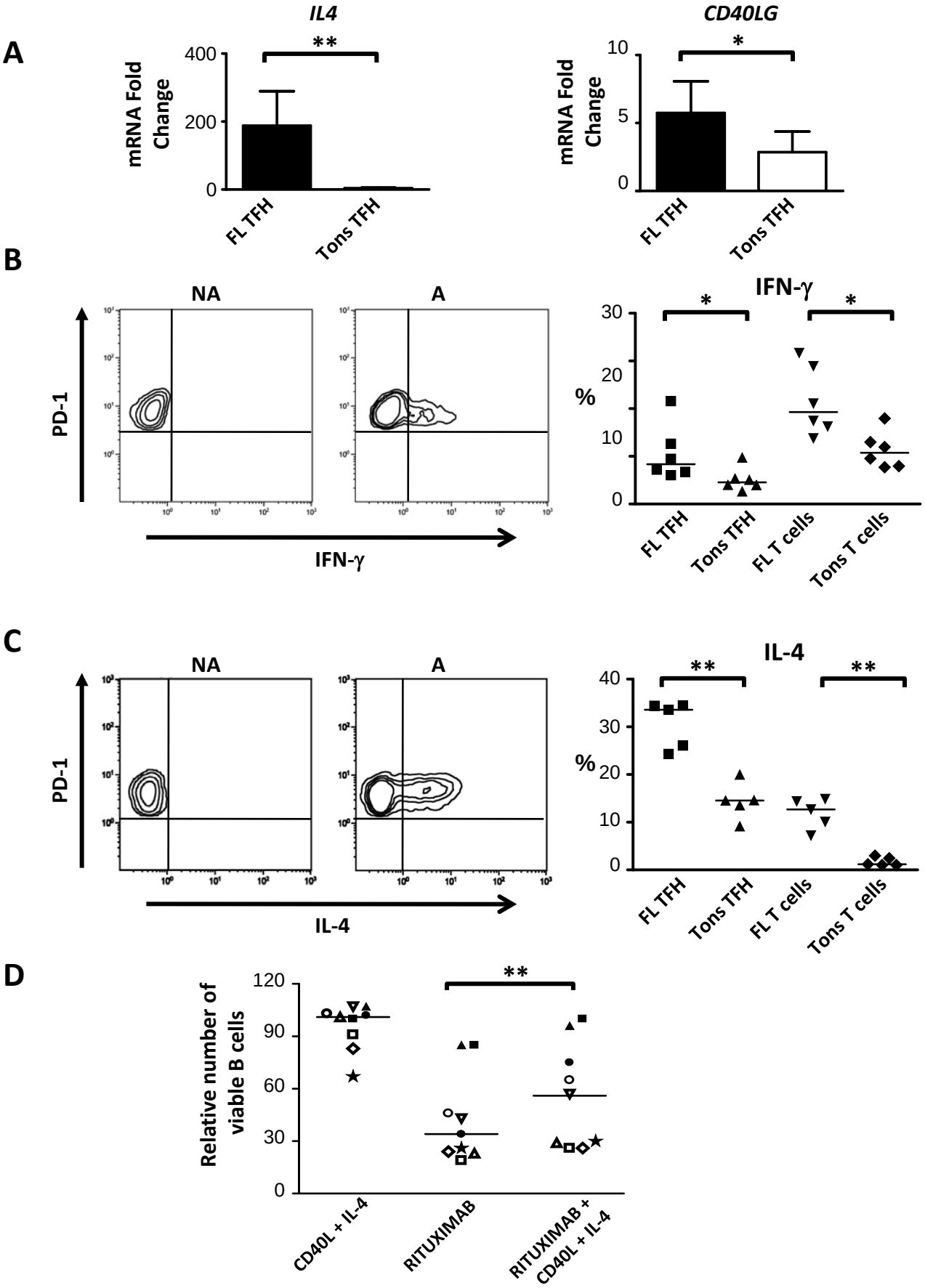
A
IL4
mRNA Fold Change
400
200
0
**
FL TFH
Tons TFH
CD40LG
mRNA Fold Change
10
5
0
*
FL TFH
Tons TFH
B
NA
A
PD-1
IFN-γ
IFN-γ
%
30
20
10
0
*
*
FL TFH
Tons TFH
FL T cells
Tons T cells
C
NA
A
PD-1
IL-4
IL-4
%
40
30
20
10
0
**
**
FL TFH
Tons TFH
FL T cells
Tons T cells
D
Relative number of viable B cells
120
90
60
30
0
**
CD40L + IL-4
RITUXIMAB
RITUXIMAB + CD40L + IL-4

Table S1: List of the genes analyzed by quantitative RT-PCR using TaqMan Gene Expression Assays

Gene symbol	Name	Unigene reference	TaqMan® Gene expression Assay Reference
18S	Eukaryotic 18S rRNA	-	Hs99999901_s1
AHR	aryl hydrocarbon receptor	Hs.171189	Hs00169233_m1
B2M	beta-2-microglobulin	Hs.534255	Hs99999907_m1
BCL6	B-cell CLL/lymphoma 6	Hs.478588	Hs00277037_m1
BTLA	B and T lymphocyte associated (CD272)	Hs.445162	Hs00699198_m1
CASC3	cancer susceptibility candidate 3	Hs.725173	Hs00201226_m1
CCR4	chemokine (C-C motif) receptor 4	Hs.184926	Hs99999919_m1
CCR6	chemokine (C-C motif) receptor 6	Hs.46468	Hs00171121_m1
CCR7	chemokine (C-C motif) receptor 7	Hs.370036	Hs00171054_m1
CCR8	chemokine (C-C motif) receptor 8	Hs.113222	Hs00174764_m1
CD200	CD200 molecule	Hs.79015	Hs01033303_m1
CD40LG	CD40 ligand (CD154)	Hs.592244	Hs00163934_m1
CTLA4	cytotoxic T-lymphocyte-associated protein 4 (CD152)	Hs.247824	Hs00175480_m1
CXCL13	chemokine (C-X-C motif) ligand 13	Hs.100431	Hs00757930_m1
CXCR3	chemokine (C-X-C motif) receptor 3	Hs.198252	Hs00171041_m1
CXCR5	chemokine (C-X-C motif) receptor 5	Hs.113916	Hs00173527_m1
CYP1A1	cytochrome P450, family 1, subfamily A, polypeptide 1	Hs.72912	Hs00153120_m1
ENTPD1	ectonucleoside triphosphate diphosphohydrolase 1 (CD39)	Hs.576612	Hs00169946_m1
FOXP3	forkhead box P3	Hs.247700	Hs00203958_m1
GATA3	GATA binding protein 3	Hs.524134	Hs00231122_m1
ICOS	inducible T-cell co-stimulator (CD278)	Hs.56247	Hs00359999_m1
IFNG	interferon, gamma	Hs.856	Hs00174143_m1
IL10	interleukin 10	Hs.193717	Hs99999035_m1
IL13	interleukin 13	Hs.845	Hs00174379_m1
IL17A	interleukin 17A	Hs.41724	Hs00174383_m1
IL17F	interleukin 17F	Hs.272295	Hs00369400_m1
IL2	interleukin 2	Hs.89679	Hs00174114_m1
IL21	interleukin 21	Hs.567559	Hs00222327_m1
IL22	interleukin 22	Hs.287369	Hs00220924_m1
IL25	interleukin 25	Hs.302036	Hs00224471_m1
IL26	interleukin 26	Hs.272350	Hs00218189_m1
IL27	interleukin 27	Hs.528111	Hs00377366_m1
IL4	interleukin 4	Hs.73917	Hs00174122_m1

LTA	lymphotoxin alpha (TNF superfamily, member 1)	Hs.36	Hs00236874_m1
LTB	lymphotoxin beta (TNF superfamily, member 3)	Hs.376208	Hs00242737_m1
MAF	v-maf musculoaponeurotic fibrosarcoma oncogene homolog	Hs.134859	Hs00193519_m1
MME	membrane metallo-endopeptidase (CD10)	Hs.307734	Hs00153510_m1
OSM	oncostatin M	Hs.248156	Hs00171165_m1
PDCD1	programmed cell death 1 (CD279)	Hs.158297	Hs00169472_m1
PRDM1	PR domain containing 1, with ZNF domain	Hs.436023	Hs00153357_m1
RC3H1	ring finger and CCCH-type zinc finger domains 1	Hs.30258	Hs02577215_m1
RORA	RAR-related orphan receptor A	Hs.560343	Hs00536545_m1
RORC	RAR-related orphan receptor C	Hs.256022	Hs01076112_m1
SH2D1A	SH2 domain protein 1A	Hs.349094	Hs00158978_m1
TBX21	T-box 21	Hs.272409	Hs00203436_m1
TGFB1	transforming growth factor, beta 1	Hs.645227	Hs99999918_m1
TNF	tumor necrosis factor (TNF superfamily, member 2)	Hs.241570	Hs00174128_m1
TNFRSF18	tumor necrosis factor receptor superfamily, member 18	Hs.212680	Hs00188346_m1

Table S2: Antibodies used for flow cytometry

Anti-human antibody	Conjugation*	Supplier**
Caspase 3	PE	BD
CD2	PC7	BC
CD3	ECD	BC
CD4	FITC	BC
CD4	PC7	BC
CD19	FITC	BC
CD20	FITC	BC
CD25	APC	BD
CD25	PC5.5	BD
CD25	PC7	BD
CD57	FITC	BC
CD86	PE	BC
CD127	A647	BD
CD200	A647	S
CXCR5	PE	RD
FOXP3	PE	EB
ICOS	BIOT	EB
IFN-γ	PE	BD
IL-4	PE	BD
kappa	FITC	BC
lambda	FITC	BC
PD-1	A647	EB
PD-1	FITC	EB

* FITC: fluorescein isothiocyanate; PE: phycoerythrin; PC5.5: phycoerythrin cyanin 5.5; PC7: phycoerythrin cyanin 7; APC: allophycocyanin; ECD: energy-coupled-dye; A647: AlexaFluor 647; BIOT: biotinylated monoclonal antibody (revealed by streptavidin-ECD, PC5 or PC7 from Beckman Coulter)

** BC: Beckman Coulter (Fullerton, CA); BD: BD Biosciences (San Diego, CA); EB: eBioscience (San Diego, CA); RD: R&D Systems (Abingdon, UK); S: AbD Serotec (Oxford, UK).